

1 ANALYSIS OF MICROBIAL COMMUNITY DURING BIOFILM DEVELOPMENT IN AN
2 ANAEROBIC WASTEWATER TREATMENT REACTOR

3

4 Nuria Fernández, Emiliano Enrique Díaz, Ricardo Amils, and José L. Sanz*

5

6 Department of Molecular Biology, Universidad Autónoma de Madrid, Madrid, 28049 Spain.

7

8

9 Running title: Biodiversity and structure of anaerobic biofilms

10

11 Corresponding author:

12 José L. Sanz. Dpto. de Biología Molecular, Universidad Autónoma de Madrid, Campus de

13 Cantoblanco, Ctra. de Colmenar, Km.15, Madrid, C.P.: 28049

14 Tel.: +34 91497 8078; fax: +34 91497 8087.

15 E-mail address: joseluis.sanz@uam.es

16

17

* Corresponding author: Dpto. de Biología Molecular, Universidad Autónoma de Madrid,
Campus de Cantoblanco, Ctra. de Colmenar, Km.15, Madrid, C.P.: 28049
Tel.: +34 91497 8078; fax: +34 91497 8087.
E-mail address: joseluis.sanz@uam.es

18 **ABSTRACT**

19 The formation, structure and biodiversity of a multispecies anaerobic biofilm inside an Upflow
20 Anaerobic Sludge Bed (UASB) reactor fed with brewery wastewater was examined using
21 complementary microbial ecology methods such as Fluorescence in situ Hybridization,
22 Denaturing Gradient Gel Electrophoresis and cloning. The biofilm development can be roughly
23 divided into three stages: an initial attachment phase (0-36 hours) characterised by random
24 adhesion of the cells to the surface; a consolidation phase (from 36 hours to 2 weeks) defined by
25 the appearance of microcolonies; and maturation phase (from 2 weeks to 2 months). During the
26 consolidation period proteobacteria with broad metabolic capabilities, mainly represented by
27 members of alpha-*Proteobacteria* class (*Oleomonas*, *Azospirillum*), predominated. Beta-,
28 gamma-, delta- (both syntrophobacteria and sulfate-reducing bacteria) and epsilon- (*Arcobacter*
29 sp.) *Proteobacteria* were also noticeable. *Archaea* first appeared during the consolidation period.
30 A *Methanospirillum*-like methanogen was detected after 36 hours and this was followed by the
31 detection of *Methanosarcina*, after four days of biofilm development. The mature biofilm
32 displayed a hill and valley topography with cells embedded in a matrix of exopolymers where the
33 spatial distribution of the microorganisms became well-established. Compared to the earlier
34 phases the biodiversity had greatly increased. Although alpha-*Proteobacteria* remained as
35 predominant, members of the phyla *Firmicutes*, *Bacteroidete* and *Thermotogae* were also
36 detected. Within the domain *Archaea*, the acetoclastic methanogen *Methanosaeta concilii*
37 become dominant. This study provides insights on the trophic web and the shifts in population
38 during biofilm development in an UASB reactor.

39

40 **Introduction**

41 Biofilms are structured microbial communities made up of groups of cells suspended in a
42 self-produced hydrated polymeric matrix of variable density and permeated by channels [13, 14].
43 In most natural and engineered environments, a multispecies microbial community is the
44 prevailing life form [58]. Although many species are implicated, biofilm development has been
45 mainly studied using systems composed by one or two species which have led the formulation of
46 a development model, in which the formation of biofilms occurs in multiple steps: (i) approach of
47 microbes to a surface, (ii) initial attachment mainly governed by van der Waals and electrostatic
48 forces; (iii) formation of microcolonies; and (iv) biofilm maturation in which microcolonies are
49 stabilized by increased cell-surface adhesion due to the accumulation of extracellular polymer
50 substance (EPS) [21, 51, 57, 58]. Mature biofilms show a complex structure (the mushroom or
51 the tulip model) with extensive presence of extracellular polymeric substances (EPS) full of
52 channels through which a liquid phase is free to move [34, 60].

53 Biofilms play an important role in wastewater treatment as they form the basis of diverse
54 aerobic and anaerobic reactors (trickling filters, rotating biological contactors...) and are
55 characterized by their feasibility and efficiency. Pollutants are anaerobically processed and
56 eliminated by means of the complex food chain established within the biofilm [30]. Consequently,
57 the process efficiency is the result of the biofilm microbial diversity. Nevertheless, studies of
58 biofilm growth in wastewater treatment systems have focused mainly on the influence of
59 operational parameters, physicochemical factors and the properties of the supports on biofilm
60 development [26, 56]. On the other hand, activity, adhesion, biomass and other conventional
61 parameters have been measured to assess the microbial community [22, 29, 52]. Reports based
62 on microbial ecology techniques are scarce [8, 19, 49].

63 Conventional cultivation-dependent microbiological techniques fail to give an indication of
64 biodiversity (about 99% of the bacterial cells in biofilms can not be cultured on standard media
65 [60]) or the architecture of a biofilm. During the last 15 years, molecular techniques based on

66 16S rRNA/rDNA have been successfully applied to microbial ecology research. Denaturing
67 Gradient Gel Electrophoresis (DGGE) [39, 40], Fluorescence in situ Hybridization (FISH) [7, 50,
68 54], together with molecular cloning, have opened up new perspectives for the study of microbial
69 ecosystems [5]. FISH combined with Confocal Laser Scanning Microscopy (CLSM) makes it
70 possible to study biofilms in natural [34], industrial [35] and engineered [15] environments
71 without destroying their critical architecture. An excellent review of the application of molecular
72 ecology techniques to wastewater treatment systems has recently been published [42].

73 The aim of this study was to investigate in detail the formation of a multispecies
74 anaerobic biofilm inside a reactor. The Upflow Anaerobic Sludge Bed (UASB) reactor was
75 chosen as it is widely used throughout the world. Scanning electron microscopy (SEM) and
76 CLSM combined with FISH were used to monitor the development and structure of the biofilm.
77 Biodiversity was evaluated with three rRNA-based complementary methods: FISH, DGGE and
78 cloning and sequencing of 16S rDNA.

79

80 **Methods**

81 Experimental set-up: A laboratory scale UASB reactor (0.9 L) was operated for five
82 months. Intact and crushed granular sludge (2.5 g VSS L⁻¹) from a full-scale UASB reactor
83 treating brewery wastewater (MAHOU, Guadalajara, Spain) was used as inoculum. The reactor
84 was fed with industrial wastewater from a brewery (4000 mg L⁻¹ COD; 2400 mg l⁻¹ BOD; 1.3 g
85 L⁻¹ TSS; 100 mg l⁻¹ TNK; 15 mg L⁻¹ NH₄⁺, 15 mg L⁻¹ P) pH 7.0, and operated with a hydraulic
86 retention time of 24 hours at 30°C. The typical composition of brewery wastewater is (in mM per
87 g of COD): 1.6 acetate, 1 propionate, 6-8 ethanol, and less than 0.2 of butyrate, lactate,
88 succinate and glucose. The VFA in the effluent after UASB treatment is around 10% of their
89 content in the effluent (23, 61).

90 Once the reactor reached steady state (organic loading rate: 1 g-COD L⁻¹ d⁻¹; sludge
91 loading rate 0.35 g-COD g-VSS⁻¹ d⁻¹; efficiency of COD removal: 85-90%, no volatile fatty acids
92 accumulated), biofilms were allowed to develop on vertical glass slides submerged in the
93 reactor.

94
95 *Growth curve:* Once the reactor reached steady state, a growth curve during the 10 first
96 days of biofilm development was obtained to provide insights on the initial period of biofilm
97 development. At the beginning of the experiment, several Falcon 3911 MicroTest III assay plates
98 were vertically placed inside the reactor. Subsequently three of them were removed at each
99 sampling time. The biofilm formation was determined by optical density at 560 nm as previously
100 described [25]

101
102 *Fluorescent in situ hybridization (FISH):* Supports consisting glass slides with 10-wells
103 (75X25 mm, with wells of 5 mm diameter) (Superior, Marienfeld, Germany) were hung vertically
104 by a nylon line at a distance of a few centimetres over the sludge bed. All the slides were
105 introduced at the start of the biofilm formation experiment and they were removed at different

106 times (1, 2, 4, 12, 24 and 36 hours, and 2, 4, 8, 18, 25, 30 and 60 days) for *in situ* hybridization.
107 Samples were rinsed with filtered water to remove loosely attached planktonic forms and
108 immediately fixed with ethanol for Gram-positive bacteria detection or with 4% paraformaldehyde
109 in phosphate buffered saline solution (PBS) during 4 hours at 4 °C for Gram-negative bacteria.
110 The samples were then washed in PBS, and stored in PBS: Ethanol (1:1) solution at –20°C. All
111 samples were further dehydrated by immersion in 50%, 80% and 100% ethanol solutions for
112 three minutes each time. Hybridization was performed following the protocol described
113 elsewhere [6, 32]. The probes used in this work are listed in Table 1. The NON338 probe was
114 used as negative control. The total cells present in the samples were determined by direct
115 counting of 4',6'-diamin phenylindol (DAPI, 1mg/ml) stained cells when possible. Samples were
116 examined under a Zeiss Axiovert 200 microscope. Structural and morphological studies on intact
117 biofilms were carried out with a Confocal Radiance 2000 scanning system coupled to a Zeiss
118 Axiovert S100 TV confocal laser-scanning microscope.

119
120 *Scanning electron microscopy (SEM):* Samples for scanning electron microscopy were
121 prepared as follows: biofilms were grown on glass slides (Φ 0.5 cm, FEDELCO, ER-308). The
122 location of the slides and sampling protocol were similar to FISH procedure. Once a sample was
123 taken out from the reactor it was fixed with glutaraldehyde (2.5% v/v) in 0.2 M sodium cacodylate
124 buffer (pH 7.1) and dehydrated with graded ethanol solutions (10%, 30%, 50%, 70%, 90% and
125 100% ethanol). The samples were dehydrated by the critical point drying method and coated
126 with gold. Micrographs were taken with a Phillips XL30 EDAX DX4i SEM.

127
128 *DNA extraction and 16S rRNA amplification:* Two- and 60-day old biofilms were detached
129 from the slides using Triton X-100 (0.25%) solution. DNA was extracted using FastDNA kit for
130 soils BIO101 according to the manufacturer's protocol. The 16S rRNA genes from mixed
131 microbial DNA were amplified by PCR. To obtain almost complete 16S rRNA gene, two

132 oligonucleotide primer pairs were used: 27F and 1492R (annealing T: 56°C) for the domain
133 *Bacteria* [28] and 25F and 1492R (annealing T: 52 °C) for the domain *Archaea* [28]. For
134 subsequent DGGE analysis, a fragment of DNA was amplified with two primer pairs: 341F-GC
135 and 907R (annealing T: 52 °C) for the domain *Bacteria* [11] and 622F-GC and 1492R (annealing
136 T: 42°C) for the domain *Archaea* [12] (GC clamp: 5'-CGC CCG CCG CGC CCC GCG CCC GTC
137 CCG CCC CCG CCC-3'). PCR reactions were performed with the following thermocycler
138 program: pre-denaturation at 94 °C for 5 min, 30 cycles of denaturation at 94 °C for 1 min,
139 annealing at corresponding temperature for 1 min, and elongation at 72 °C for 3 min (1 min for
140 DGGE use); and post-elongation at 72 °C for 10 min.

141
142 *Denaturing Gradient Gel Electrophoresis (DGGE):* The PCR products of the same length
143 were separated by DGGE [36], which was performed according to the Dcode-System (BioRad,
144 Germany). Polyacrylamide gels 6% (wt/vol, acrylamide-bisacrylamide 37.5:1) were prepared
145 with denaturing gradients ranging from 30% to 60% (in which 100% denaturant contained 7M
146 urea and 40% v/v formamide) and were run at 60°C and 80V for 15 h. Bands detected by
147 fluorescence using a UV transilluminator were excised and re-amplified for sequencing.

148
149 *Clone libraries, ARDRA analysis and sequencing:* For a further comparison between
150 young and mature biofilm communities, two- and 60-day old biofilms were analyzed by clone
151 libraries. The 16S rRNA gene amplicates (length 1465 and 1467 bp for *Bacteria* and *Archaea*,
152 respectively) were cloned using TOPO Cloning Kit (Invitrogen Corporation, San Diego,
153 California) and then transformed into competent *E. coli* cells. Plasmid inserts were screened by
154 Amplified Ribosomal DNA Restriction Analysis (ARDRA) using the enzyme *Sau3AI* (BioLabs
155 Inc., New England). Fragments were separated by 2% (w/v) agarose (Pronadisa, Madrid) gel
156 electrophoresis and visualized by ethidium bromide staining. Clones were grouped according to
157 their restriction patterns defining different Operational Taxonomic Units (OTUs). Subsequently,

158 two clones of each OTU were amplified by PCR using the M13 primer set (Invitrogen).
159 Automated DNA sequencing was performed with an ABI model 377 sequencer (Applied
160 Biosystems).

161
162 *Sequence analysis:* All sequences obtained in this work were compared with the
163 databases by using Basic Local Alignment Search Tool (BLAST) [1] to identify the closest
164 sequence. Sequence data were aligned and analyzed with the ARB program package [31].
165 Parsimony was used to construct phylogenetic trees.

166
167 *Nucleotide sequence accession numbers:* The sequences obtained in this study have
168 been deposited in the GenBank database under accession numbers AY692039 to AY692074.

169

170 **Results**

171 Three complementary approaches were used to monitor the kinetics of biofilm formation,
172 their phylogenetic diversity, and the spatial distribution of the populations: SEM, FISH and DNA
173 sequencing after direct cloning of the 16S rRNA gene as well as resolution by DGGE of
174 amplified fragments of this gene.

175

176 *SEM:* Microscopic examination showed an erratic colonization sequence during the first
177 few hours of biofilm formation. The cell density on the surface changed continuously without a
178 trend and the microorganisms were widely spaced on the surface of the support (Fig. 1, 3h-24h).
179 After two days, the growth tended to stabilize, the production of a matrix of exopolymers began
180 and the first microcolonies could be observed (Fig 1, 4d). The microcolonies then progressively
181 spread to form a biofilm (Fig. 1, 8d-14d). SEM images showed that the mature biofilm consisted
182 of both densely populated and less dense areas during the growth period (Fig. 1, 60d), results
183 that were similar to those previously reported [52].

184 These data were corroborated by monitoring the adhered cells during the first 10 days
185 (Fig. 2). The growth curve showed that adhesion behaviour was random during the first 36
186 hours, corresponding to the period before growth of microcolonies was observed by SEM.
187 Subsequently, a constant rate of adhesion was observed which tended to stabilize in the final
188 stage of the studied period.

189 This microscopic analysis also revealed extensive morphological diversity including
190 different kinds of spirillum, straight and curved rods and small coccoid cells (Fig. 1, 4d detail).
191 Two methanogens could be identified due to their particular shape: *Methanospirillum*-like cells
192 appeared after one day of growth whereas *Methanosaeta*-like cells were clearly identified after
193 four days.

194
195 *FISH*. Based on SEM and growth curve results, to determine the spatial distribution of
196 the microorganisms the development of the biofilm was divided roughly into three stages: initial
197 attachment (0-36 hours), consolidation (from 36 hours to 2 weeks) and maturation (from 2 weeks
198 to 2 months).

199 Different groups belonging to the domain *Bacteria* (α , β , γ -*Proteobacteria*,
200 *Syntrophobacter*, sulfate-reducing bacteria, *Bacteroides* and Gram-positive bacteria) were
201 analyzed by FISH and quantified for each stage. During initial attachment, the number of
202 microorganisms reached 10^6 cells/cm² (total DAPI stained cells), with a percentage of hybridized
203 cells between 50-70% (probes EUB338 plus ARC915 versus DAPI stained cells). Of those, 85-
204 95% corresponded to the domain *Bacteria*. During this period, α -*Proteobacteria* (35-55% of
205 detected bacterial cells, Fig. 3A) was the most representative group. β - and γ -*Proteobacteria* (5-
206 15% each) were also detected, always associated to colonies of α -*Proteobacteria* (Fig. 3B and
207 3C). The presence of *Syntrophobacter* (5-10%) and sulfate-reducing bacteria (5-8% each) was
208 also noticeable (Fig. 3D and 3E). The presence of archaea could be detected after only 36
209 hours, although these microorganisms were always scarce in comparison to bacteria. These

210 cells had the form of long bowed rods that formed small *Methanospirillum*-like filaments, which
211 hybridized with the MG1200 (*Methanomicrobiales*) probe (Fig. 3F), confirming the results of
212 SEM.

213 The consolidation stage of the biofilm was marked by the formation of colonies that
214 began to interconnect but still appeared as independent entities (Fig. 3H). β -*Proteobacteria* were
215 specifically located on the edges of the colonies. These colonies were mainly made up of α -
216 *Proteobacteria* together with the other groups detected: γ -*Proteobacteria*, *Syntrophobacter* and
217 sulfate-reducing bacteria which had not a tendency to occupy specific positions within the
218 colonies. Archaea were basically represented by *Methanospirillum*-like cells (probe MG1200:
219 *Methanomicrobiales*), as large rods and small filaments scattered throughout the bacterial
220 colonies forming a network. *Methanosarcina* genus (probe MS1414) were observed after four
221 days of growth, making up dense packed within the bacterial colonies (Fig. 3H and 3I), although
222 in smaller amounts than *Methanospirillum*-like cells. In addition to this *Methanobacteriales* group
223 (probe MEB859, Fig. 3G) was found in very small quantities. The presence of *Methanosaeta*
224 was not detected.

225 Mature biofilm covered almost the entire surface of the support, with cells embedded in
226 an exopolymeric matrix. 3D reconstructions based on biofilm sections obtained using confocal
227 microscopy revealed their spatial distribution. The groups detected were not very different from
228 previous stages. The main body was formed mostly of bacteria, with the archaeal cells clearly
229 defined within it (Fig. 3J). They were basically α -*Proteobacteria*, with β -*Proteobacteria* always
230 located on the edge of the biofilm and γ - and δ -*Proteobacteria* scattered within it. *Bacteroides*
231 and Gram-positives were also detected at this stage. Archaea appeared as individual cells or
232 short filaments that spread forming a network throughout the biofilm; however, it was mainly
233 composed of *Methanosaeta* filaments. It appears that *Methanospirillum* was displaced by
234 *Methanosaeta*. As noted before, densely packed groups of very bright *Methanosarcina* were
235 normally located inside the colonies (Fig. 3J).

236

237 *DGGE profiles:* Changes in microbial diversity during biofilm formation were studied
238 using DGGE profiling. Figure 4 shows the band patterns resolved with DGGE after partial 16S
239 rRNA gene amplification using specific primers for the domains *Archaea* and *Bacteria*. *Archaea*
240 were not detected during the first 24 hours of development. Since then and during the rest of the
241 studied period, a stable pattern was maintained for this domain (Fig. 4A). The bacterial patterns
242 were highly variable during the first two days reflecting large changes in diversity in this domain
243 at the beginning of the growth (Fig. 4B). After that, the bacterial diversity remained fairly
244 constant.

245 All visible bands were excised from the DGGE fingerprints, re-amplified, purified and
246 sequenced. A total of eleven bacterial bands and three archaeal bands yielded sequences that
247 were analyzed using the BLAST program. The taxonomic affiliations of the 16S rRNA partial
248 sequences are shown in Table 2. All sequenced bacterial bands belonged to *Proteobacteria*,
249 *Firmicutes*, *Actinobacteria* and *Bacteroidetes* phyla. Some of them were present only during the
250 initial period: B5 (*Flavobacteriaceae*), B7 (*Hydrogenophilaceae*) and B11 (*Nocardiaceae*). Bands
251 B2 (*Acetobacteraceae*), B3 (*Rhodocyclaceae*), B9 (*Syntrophomonadaceae*) and B10
252 (*Campylobacteraceae*) were also detected in the consolidation period. The remaining bands
253 were found in the consolidation and mature stage: B4 (*Comamonadaceae*), B1
254 (*Syntrophobacteraceae*), B6 and B8 (order *Clostridiales*). In the case of the domain *Archaea*,
255 the bands belonged to *Methanosarcinales* (A1 and A2) and *Methanomicrobiales* orders from the
256 *Methanomicrobia* class.

257

258 *Clone libraries.* Two specific periods during the biofilm formation were studied by cloning: after
259 two days, at the beginning of the consolidation stage when the microorganisms can be
260 considered to be specifically attached to the support, and after two months, when the biofilm is
261 mature. Almost complete 16S rRNA sequences were amplified from total DNA extracted from

262 the biofilm using universal primers for the bacterial and archaeal domains. ARDRA analysis of
263 the 90 (bacterial Domain) and 85 (archaeal Domain) clones for the two day-old biofilm and 77
264 (bacterial Domain) and 96 (archaeal Domain) clones for the sixty days-old biofilm allowed us to
265 group them and to define different Operational Taxonomic Units (OTUs) which were formed from
266 clones with the same restriction band pattern (Table 2).

267 After two days of biofilm formation, 5 different OTUs were detected for *Bacteria* domain
268 and 1 for *Archaea* domain, while after 60 days, 6 and 3 OTUs were found, respectively. The 16S
269 rRNA gene sequences were affiliated with mainly uncultured bacteria from different habitats and
270 only remotely related to known bacterial species (Table 3).

271 Taxonomic similarities and phylogenetic relationships showed that most of the bacteria
272 belonged to the phylum *Proteobacteria* (Table 3, Fig. 6): two OTUs could be included in the α
273 class, one was related to *Acetobacteraceae* (Cb1) and the other to *Rhodospirillaceae* (Cb2);
274 another one in the β class was related to *Rhodocyclaceae* (Cb3); one OTU in the δ class was
275 related to sulfate-reducing bacteria (Cb4); and one OTU in the ε class was related to the
276 *Arcobacter* genus (Cb5). Many of the remaining sequences were members of Gram-positive
277 bacteria: three OTUs belonging to the *Clostridiales* (Cb6, Cb7 and Cb8). Members of the
278 *Flavobacterium-Cytophaga* group (Cb9) and *Thermotogae* phylum (Cb10) were also identified.

279 Three methanobacteria were identified inside the domain *Archaea* (Table 3, Fig. 6). Two
280 could be included in the *Methanosarcinales* order: *Methanosaeta* (Ca1 and Ca2) and
281 *Methanosarcina* genera (Ca3). The other sequences belonged to the *Methanomicrobiales* order,
282 probably to the *Methanospirillum* genera (Ca4).

283

284 **Discussion**

285 The main phases described for single-species biofilm formation were also observed
286 during the development of a multispecies anaerobic biofilm. It is known that microbial cells might
287 be affected by the adsorption-desorption processes caused by the electrostatic and shearing

288 forces that take place between a surface charges and charges on the bacterial surface [30]. This
289 could explain the behavior observed during the initial stage of development in which the
290 microbial adhesion to the support was a random process, as indicated by SEM (Fig. 1) and
291 supported by optical density measurements (Fig. 2), FISH (Fig. 3 A, to F) and the band patterns
292 generated with DGGE (Fig. 4). In this study, the influence of physicochemical and operational
293 conditions on the growth trend was minimized since the reactor was operated at steady-state
294 throughout the entire experiment and the environmental conditions were expected to be fairly
295 constant. It should be noted that neither archaea nor Gram-positive bacteria appeared during the
296 first 36 hours. It is plausible that the chemical characteristics of their external envelopes, and the
297 lower number of fimbriae of Gram-positive with respect to the Gram-negative bacteria could be
298 critical factors during the initial colonization and could be implicated in their delay in colonizing
299 the surface.

300 According to the accepted model, once beyond this initial stage, the influence of the
301 stochastic processes and physicochemical conditions waned and the nature of the bacteria-
302 surface interaction could be determined by the attachment of bacterial fimbriae [18] and by the
303 excretion of an exopolymeric matrix [18, 53]. Such a matrix was observed after 1-2 days and
304 marked the beginning of the consolidation stage. From this point on the physical structure of
305 biofilm evolved, changing from isolated microcolonies to a mature stage in which the cells were
306 embedded in the matrix, adopting rounded shapes stabilized by EPS (Fig. 1, 60th day). In
307 addition, the bacterial diversity of the biofilm, confirmed by FISH and DGGE band patterns,
308 remained fairly constant in comparison with the initial stage. This implies that the basis of the
309 microbial community and therefore the main pathways of the trophic web were formed during the
310 consolidation stage.

311 Once irreversible adhesions to the surface had occurred and the microcolonies started to
312 form, the first community mainly comprised α -*Proteobacteria* according to FISH. *Oleomonas*
313 *sagaranensis* (Cb1, B2) is able to form aggregates [27] producing some EPS, so facilitating its

314 adhesion to the surface. This characteristic and its high metabolic versatility [27]—are
315 advantages that make this microorganism a pioneer in the colonization of the surface. At the
316 same time *Azospirillum* (Cb2), which also has a broad metabolic capability, appeared. These
317 two α -*Proteobacteria* could participate in the breakdown of organic polymers.

318 In general, the microorganisms that initiated the formation of the biofilm have a broad
319 metabolic flexibility that facilitated invasion of the surface. The intermediates produced after the
320 lysis of macromolecules could be degraded by proteobacteria: *Oleomonas* (Cb1, B2), *Azonexus*
321 (B3), *Azospirillum* (Cb2), a γ -*Proteobacteria* (enterobacteria were detected by FISH), *Arcobacter*
322 (Cb5, B10), or sulfate reducers (FISH data) [10], or by the firmicutes *Thermovirga* (B9).
323 *Syntrophobacteria* (B1) was a expected member of the microbial community because it is
324 implicated in the degradation of fatty acids and others intermediate products during fermentation
325 to acetate and hydrogen. However *Syntrophobacteria* appeared in low proportions (FISH data)
326 in the first stages. We must emphasize that *Azonexus* is able to grow under microaerophilic
327 conditions, in line with the observation that the β -*Proteobacteria* were always located in the
328 exterior zones of the microcolonies where they had access to traces of oxygen present in the
329 reactor. The presence of a microorganism related to the class *Flavobacteria* (Cb9, B5) seems
330 odd because they are typical of aerobes environments. Nonetheless, sequences similar to
331 *Cytophaga* have been found in anaerobic environments such as sulfate-reducing enrichment
332 cultures [41] and in granular sludge [12]. It has been suggested that the *Cytophaga*-
333 *Flavobacterium* cluster play an important role in the degradation of complex organic matter in
334 anaerobic marine sediments [45]. This role might be extended to all anaerobic environments.

335 According to the FISH results, major microbial groups within the biofilm maintained the
336 same architecture during biofilm maturation. Nevertheless, with time, new members appeared
337 thus increasing the complexity of the ecosystem. In the maturation stage, some new sequences
338 were retrieved (Cb6, Cb7, Cb8, B6, B8). Based on the closest genus described
339 (*Aminobacterium*, *Catabacter* and *Clostridium*), these sequences belong to the Gram-positive

340 class *Clostridia*, which together with *Bacteroidetes* members (FISH data) could be involved not
341 only in hydrolysis and but also in fermentation steps. Some closely related sequences have
342 been found in methanogenic sludge (AF323770, not published) and granular sludge [16],
343 suggesting that these microorganisms are extremely widespread in anaerobic systems and that
344 they must have an important role in anaerobic digestion Even though, an interesting observation
345 was that microorganisms from the phylum *Thermotogae* were detected in the mature biofilm.
346 Mesophilic *Thermotogae* have been isolated from anaerobic ecosystems [37, 59] and also
347 several similar sequences have been reported in an anaerobic reactor (AB195923, not
348 published).

349 With regard to the domain *Archaea*, all microorganisms identified in the biofilm
350 corresponded to methanogenic archaea. They were absent until 36 hours of biofilm
351 development. During the consolidation stage, the number of methanogens grew in parallel with
352 increase in microcolony size, mainly represented by *Methanospirillum* sp., a hydrogenotrophic
353 methanogen that began to form an increasingly complex network within the bacterial colonies
354 (FISH data, A3). Because of the energy released, the biomass yield is lower for acetate-
355 consuming methanobacteria than for hydrogen-consumers favoring initial predominance
356 of *Methanospirillum* over *Methanosarcina* and *Methanosaeta*. The increased number of
357 fermentative microorganisms implied a higher availability of acetate for acetoclastic
358 methanogens, which appeared later than hydrogenotrophic ones. The first acetoclastic
359 methanogen to appear was the genus *Methanosarcina* (Ca3,A1), which was found in the biofilm
360 as dense, bright packs. In the case of granular sludge, it has been reported [20] that substrates
361 that are easily fermented—such as the brewery wastewater used to feed our reactor—are
362 degraded mainly on the surface of granular sludge, while the intermediate products are
363 converted into acetate in the middle layers. This would explain the position in the biofilm of
364 *Methanosarcina*, which has a high K_s (4.02 mmol L⁻¹) for acetate. DGGE and clone libraries
365 showed the presence of *Methanosaeta* genus (Ca1, Ca2, A2) in the former steps but it was

366 impossible to detect by FISH. This implies that few of these microorganisms were present (less
367 than 1%) but their metabolic role was negligible.

368 In the evolution to a mature biofilm, *Methanospirillum hungateii*, was displaced over time
369 by *Methanosaeta concilii*. This archaea is the dominant methanogen in the anaerobic granular
370 sludge reactors [2, 47, 48]. which was used to inoculate our reactor. *M. concilii* is an exclusively
371 acetoclastic organism with a slow growth rate ($V_{max} = 0.11 \text{ d}^{-1}$). This could explain its early
372 detection by means of PCR-based technologies whereas with FISH it only appeared in
373 abundance in the mature stages of the biofilm. It is well known [33] that the complexity of the
374 trophic web of an engineered ecosystem leads to the prevalence of acetate over hydrogen as
375 the final product of the fermentation, resulting in overgrowth of *Methanosaeta* compared to
376 *Methanospirillum*.

377 The techniques based on the 16S rRNA gene allowed us to describe the development
378 and diversity in the microbial community of an anaerobic biofilm. The insight gained on the
379 formation of biofilms during anaerobic wastewater treatment can be applied to control anaerobic
380 bioreactor technology for a wide range of applications.

381

382 **Acknowledgments**

383 This work was supported by grant CTM2006-04131/TECNO from the Spanish Ministry of
384 Education and Science. The CBM is also indebted to an institutional grant from the Fundación
385 Areces.

386

387 **References**

388 [1] Altschul SF, Gish W, Miller W, Myers EW & Lipman DJ (1990) Basic local alignment
389 search tool. J Mol Biol 215: 403-410

390 [2] Alphenaar PA (1994) Anaerobic granular sludge: characterization, and factors affecting
391 its functioning. Ph.D. thesis, Landbouwniversiteit, Wageningen, The Netherlands

- 392 [3] Amann RI, Krumholz I, Stahl DA (1990) Fluorescent oligonucleotide probing of whole
393 cells for determinative, phylogenetic, and environmental studies in microbiology. *J*
394 *Bacteriol* 172: 762-770
- 395 [4] Amann RI, Binder BJ, Olson BJ, Chisholm SW, Devereux R, Stahl DA (1990)
396 Fluorescent-oligonucleotide probing of whole cells for determinative, phylogenetic, and
397 environmental studies in microbiology. *J Bacteriol* 172: 762-770
- 398 [5] Amann RI, Ludwig W, Schleifer KH (1995) Phylogenetic identification and in situ
399 detection of individual microbial cells without cultivation. *Microbiol Rev* 59: 143-169
- 400 [6] Amann RI (1995) In situ identification of micro-organisms by whole cell hybridization
401 with rRNA-targeted nucleic acid probes. In: Akkermans ADL, van Elsas JK (eds)
402 *Molecular Microbial Ecology Manual*, Section 3.3.6, Kluwer Academic Publishers,
403 London, p.3.3.6/1-3.3.6/15
- 404 [7] Amann RI, Fuchs BM, Behrens S (2001) The identification of microorganisms by
405 fluorescence in situ hybridisation. *Curr Opin Biotech* 12: 231-236
- 406 [8] Araujo JC, Brucha G, Campos JR, Vazoller RF (2000) Monitoring the development of
407 anaerobic biofilms using fluorescent in situ hybridization and confocal laser scanning
408 microscopy. *Water Sci Technol* 41: 69-77
- 409 [9] Boetius A, Ravensschlag K, Schubert C, Rickert D, Widdel F, Gieseke A, Amann RI,
410 Jørgesen B, Witte U, Pfannkuche O (2000) A marine microbial consortium apparently
411 mediating anaerobic oxidation of methane. *Nature* 407: 623-626
- 412 [10] *Bergey's Manual of Systematic Bacteriology* 2nd ed. (2005) The Proteobacteria,
413 Brenner DJ, Krieg NR, Staley JT (eds), Springer.
- 414 [11] Brosius J, Dull T J, Sleeter DD, Noller HF (1981) Gene organization and primary
415 structure of a ribosomal RNA operon from *Escherichia coli*. *J Mol Biol* 148: 107-127

- 416 [12] Chan O-C, Liu W-T, Fang HHP (2001) Study of microbial community of brewery-
417 treating granular sludge by denaturing gradient gel electrophoresis of 16S rRNA gene.
418 Water Sci Technol 43: 77-82
- 419 [13] Costerton JW, Llewandowski Z, DeBeer D, Caldwell D, Korber D, James G (1994)
420 Biofilms, the customized microniche. J. Bacteriol 176: 2137-2142
- 421 [14] Costerton JW, Stewart PS, Greenberg EP (1999) Bacterial biofilms: A common cause
422 of persistent infections. Science 284: 1318-1322
- 423 [15] Díaz EE, Amils R, Sanz JL (2003) Molecular ecology of anaerobic granular sludge
424 grown at different conditions. Water Sci Technol 48: 57-64
- 425 [16] Díaz EE, Stams AJ, Amils R, Sanz JL (2006) Phenotypic properties and microbial
426 diversity of methanogenic granules from a full-scale upflow anaerobic sludge bed
427 reactor treating brewery wastewater. Appl Environ Microbiol 72: 4942-4949
- 428 [17] Doré J, Sghir A, Hannequart-Gramet G, Corthier G, Pochart P (1998) Design and
429 evaluation of a 16S rRNA-targeted oligonucleotide probe for specific detection and
430 quantification of human faecal *Bacteroides* populations. Syst Appl Microbiol 21: 65-71
- 431 [18] Dunne WM (2002) Bacterial adhesion: seen any good biofilms lately? Clin Microbiol
432 Rev 15: 155-166.
- 433 [19] Egli D, Bosshard G, Werlen C, Lais P, Siegrist H, Zehnder AJB, Van der Meer JR
434 (2003) Microbial composition and structure of a rotating biological contactor biofilm
435 treating ammonium-rich wastewater without organic carbon. Microbial Ecol 45: 419-
436 432.
- 437 [20] Fang HHP (2000) Microbial distribution in UASB granules and its resulting effects.
438 Water Sci Technol 42: 201-208
- 439 [21] Fang HHP, Chan K-Y, Xu L-C (2000) Quantification of bacterial adhesion forces using
440 atomic force microscopy (AFM) J Microbiol Meth 40: 89-97

- 441 [22] García Encina PA, Hidalgo MD (2005) Influence of substrate feed patterns on biofilm
442 development in anaerobic fluidized bed reactors (AFBR). *Process Biochem* 40: 2509-
443 2516
- 444 [23] Gonzalez-Gil G, Lens PNL, van Aelst A, van As H, Versprille AI, Lettinga G (2001)
445 Cluster structure of anaerobic aggregates of an expanded granular sludge bed reactor.
446 *Appl Environm Microb* 67: 3683-3692
- 447 [24] Harmsen HJM, Kengen HMP, Akkermans ADL, Stams AJM, De Vos WM (1996)
448 Detection and localization of syntrophic propionate-oxidizing bacteria in granular sludge
449 by in situ hybridization using 16S rRNA – based oligonucleotide probes. *Appl Environ*
450 *Microb* 62: 1656-1663
- 451 [25] Hentzer M, Teitzel GM, Balzer GJ, Heydorn A, Molin S, Givskov M, Parsek MR (2001)
452 Alginate overproduction affects *Pseudomonas aeruginosa* biofilm structure and
453 function. *J Bacteriol* 183: 5395-5401
- 454 [26] Hidalgo MD, García-Encina PA (2002) Biofilm development and bed segregation in a
455 methanogenic fluidized bed reactor. *Water Res* 36: 3083-3091
- 456 [27] Kanamori T, Rashid N, Morikawa M, Haruyuki A, Imanaka T (2002) *Oleomonas*
457 *sagaranensis* gen. nov., sp. nov., represents a novel genus in the α -*Proteobacteria*.
458 *FEMS Microbiol Lett* 217: 255-261
- 459 [28] Lane DJ (1991) 16S/23S rRNA sequencing. In: Stackebrandt E, Goodfellow M (eds)
460 *Nucleic acid techniques in bacterial systematic*, John Wiley & Sons Inc., New York, NY,
461 pp. 115-175
- 462 [29] Lehtola MJ, Miettinen IT, Keinänen MM, Kekki TK, Laine O, Hirvonen A, Vartiainen T,
463 Martikainen PJ (2004) Microbiology, chemistry and biofilm development in a pilot
464 drinking water distribution system with copper and plastic pipes. *Water Res* 38: 3769-
465 3779.

- 466 [30] Liu Y, Tay J-H (2002) The essential role of hydrodynamic shear force in the formation
467 of biofilm and granular sludge. *Water Res* 36: 1653-1665
- 468 [31] Ludwig W, Strunk O, Westram R, Richter L, Meier H, Yadhukumar, Buchner A, Lai T,
469 Steppi S, Jobb G, Förster W, Brettske I, Gerber S, Ginhart AW, Gross O, Grumann S,
470 Hermann S, Jost R, König A, Liss T, Lüßmann R, May M, Nonhoff B, Reichel B,
471 Strehlow R, Stamatakis A, Stuckmann N, Vilbig A, Lenke M, Ludwig T, Bode A,
472 Schleifer KH (2004) ARB: a software environment for sequence data. *Nucleic Acids*
473 *Res* 32:1363-1371
- 474 [32] Manz W, Amann R, Ludwig W, Wagner M, Schleifer KH (1992) Phylogenetic
475 oligodeoxynucleotide probes for the major subclasses of Proteobacteria: Problems
476 and Solutions. *Syst Appl Microbiol* 15: 593-600
- 477 [33] Manz W, Eisenbrecher M, Neu TR, Szewzyk U (1998) Abundance and spatial
478 organization of gram-negative sulfate-reducing bacteria in activated sludge investigated
479 by in situ probing with specific 16S rRNA targeted oligonucleotides. *FEMS Microbiol*
480 *Ecol* 25: 43-61
- 481 [34] Manz W, Wendt-Potthoff K, Neu TR, Szewzyk U, Lawrence JR (1999) Phylogenetic
482 composition, spatial structure, and dynamics of lotic bacterial biofilms investigated by
483 Fluorescent in Situ Hybridization and Confocal Laser Scanning Microscopy. *Microbial*
484 *Ecol* 37: 225-237
- 485 [35] McLeod ES, MacDonald R, Brözel VS (2002) Distribution of *Shewanella putrefaciens*
486 and *Desulfovibrio vulgaris* in sulphidogenic biofilms of industrial cooling water systems
487 determined by fluorescent in situ hybridisation. *Water SA* 28: 123-128
- 488 [36] Meier H, Amann RI, Ludwig W, and Schleifer KH (1999) Specific oligonucleotide
489 probes for in situ detection of a major group of gram-positive bacteria with low DNA
490 G+C content. *Syst Appl Microbiol* 22: 186-196

- 491 [37] Miranda-Tello E, Fardeau M-L, Thomas P, Ramirez F, CAsalot L, Cayol J-L, Garcia J-
492 L, Ollivier B (2004) *Petrotoga mexicana* sp. nov., a novel thermophilic, anaerobic and
493 xylanolytic bacterium isolated from an oil-producing well in the Gulf of Mexico. Int J Sys
494 Evo Microbiol 54: 169-174
- 495 [38] Mujer W, Zehnder AJB (1983) Conversion processes in anaerobic digestion. Water Sci
496 Technol 15: 127-167
- 497 [39] Muyzer G, Hottenträger S, Teske A, Wawer C (1996) Denaturing gradient gel
498 electrophoresis of PCR-amplified 16S rDNA - A new molecular approach to analyse the
499 genetic diversity of mixed microbial communities. In: Akkermans ADL, van Elsas JK
500 (eds) Molecular Microbial Ecology Manual, Section 3.4.4, Kluwer Academic
501 Publishers, London, p.3.4.4./1-3.4.4./23
- 502 [40] Muyzer G, Smalla K (1998) Application of denaturing gradient gel electrophoresis
503 (DGGE) and temperature gradient gel electrophoresis (TGGE) in microbial ecology.
504 Mini review. Anton Leeuw Int J G 73: 127-141
- 505 [41] Nakagawa T, Sato S, Yamamoto Y, Fukui M (2002) Successive changes in community
506 structure of an ethylbenzene-degrading sulfate-reducing consortium. Water Res 36:
507 2813-2823
- 508 [42] Neef A, (1997) Anwendung der in situ-Einzelzell-Identifizierung von Bakterien zur
509 populations analyse in Komplexen Mikrobiellen biozöosen. Doctoral thesis, Faculty of
510 Biology, Chemistry and Geosciences, Technische Universität München.
- 511 [43] Raskin L, Strimley J, Rittmann BE, Stahl DA (1994) Group specific 16S RNA
512 hybridization probes to describe natural communities of methanogens. Appl Environ
513 Microb 60: 1232-1240
- 514 [44] Roller E, Wagner M, Amann RI, Ludwig W, Schleifer KH (1994) In situ probing of gram-
515 positive bacteria with high DNA G+C content using 23S rRNA targeted
516 oligonucleotides. Microbiology 140: 2849-2858

- 517 [45] Roselló-Mora R, Thamdrup B, Schäfer H, Weller R, Amann R (1999) The response of
518 the microbial community of marine sediments to organic carbon input under anaerobic
519 conditions. *Sist Appl Microbiol* 22: 237-248
- 520 [46] Sanz JL, Köchling T (2007) Molecular biology techniques used in wastewater
521 treatment: An overview. *Process Biochem* 42: 119-133.
- 522 [47] Schmidt JE, Ahring BK (1995) Granular sludge formation in upflow anaerobic sludge
523 blanket (UASB) reactors. *Biotechnol Bioeng* 49: 229-246
- 524 [48] Sekiguchi Y, Kamagata Y, Nakamura K, Ohashi A, Harada H (1999) Fluorescence in
525 situ hybridization using 16S rRNA-targeted oligonucleotides reveals localization of
526 methanogens and selected uncultured bacteria in mesophilic and thermophilic sludge
527 granules. *Appl Environ Microb* 65: 1280-1288
- 528 [49] Silyn-Roberts G, Lewis G (2003) Substrata effects on bacterial biofilm development in
529 a subsurface flow dairy waste treatment wetland. *Water Sci Technol* 48: 261-269
- 530 [50] Stahl DA, Amann RI (1991) Development and application of nucleic acid probes. In:
531 Stackebrandt E, Goodfellow M (eds) *Nucleic acid techniques in bacterial systematics*,
532 John Wiley & Sons Inc, New York, pp. 205-247
- 533 [51] Tolker-Nielsen T, Brinch UC, Ragas PC, Andersen JB, Jacobsen CS, Molin S (2000)
534 Development and dynamics of *Pseudomonas* sp. biofilms. *J Bacteriol* 182: 6482-6489
- 535 [52] Thörn M, Mattsson A, Sörensson F (1996) Biofilm development in a nitrifying trickling
536 filter. *Water Sci Tech* 34: 83-89.
- 537 [53] Tsuneda S, Aikawa H, Hayashi H, Yuasa A, Hirata A (2003) Extracellular polymeric
538 substances responsible for bacterial adhesion onto solid surface. *FEMS Microbiol Lett*
539 223: 287-292
- 540 [54] Wagner M, Horn M, Daims H (2003) Fluorescence in situ hybridisation for the
541 identification and characterization of prokaryotes. *Curr Opin Microbiol* 6: 302-309

- 542 [55] Wallner, G, Amann, R, Beisker, W, 1993. Optimizing fluorescent in situ hybridization
543 with rRNA-targeted oligonucleotide probes for flow cytometric identification of
544 microorganisms. Cytometry 14, 136-143.
- 545 [56] Wäsche S, Horn H, Hempel DC (2002) Influence of growth conditions on biofilm
546 development and mass transfer at the bulk/biofilm interface. Water Res 36: 4775-4784
- 547 [57] Watnick PI, Kolter R (1999) Steps in the development of a *Vibrio cholerae* biofilm. Mol
548 Microbiol 34: 586-595
- 549 [58] Watnick P, Kolter R (2000). Minireview. Biofilm, City of Microbes. J Bacteriol 182:
550 2675-2679
- 551 [59] Wery N, Lesongeur F, Pignet P, Derennes V, Cambon-Bonavita M-A, Godfroy A,
552 Barbier G (2001) *Marinitoga camini* gen. nov., sp. Nov., a rod-shaped bacterium
553 belonging to the order *Thermotogales*, isolated from a deep-sea hydrothermal vent. Int
554 J Sys Evo Microbiol 51: 495-504
- 555 [60] Wimpenny J, Manz W, Szewzyk U (2000) Heterogeneity in biofilms. FEMS Microbiol
556 Rev 24: 661-671
- 557 [61] Wu W-M, Hickey RF, Zeikus JG (1991) Characterization of metabolic performance of
558 methanogenic granules treating brewery wastewater: role of sulphate-reducing
559 bacteria. Appl Environm Microb 57: 3438-3449
- 560

561

562

Table 1.
rDNA oligonucleotide probes used in this study

Probe	Specificity	Probe sequence (5'-3')	Reference
EUB338	<i>Bacteria</i>	GCTGCCTCCCGTAGGAGT	3
ARC915	<i>Achaea</i>	GTGCTCCCCCGCCAATTCCT	50
NON338	Negative control	ACTCCTACGGGAGGCAGC	55
ALF968	α - <i>Proteobacteria</i>	GGTAAGGTTCTGCGCGTT	42
BET42a	β - <i>Proteobacteria</i>	GCCTTCCCACATCGTTT	32
GAM42a	γ - <i>Proteobacteria</i>	GCCTTCCCACATCGTTT	32
SRB385	Sulfate-reducing bacteria	CGGCGTCGCTGCGTCAGG	3
DSS658	<i>Desulfosarcina, Desulfococcus</i>	TCCACTTCCCTCTCCCAT	33
DSV698	<i>Desulfovibrio</i> sp.	GTTCTCCAGATATCTACGG	33
SYN835	<i>Syntrophobacter</i>	GCAGGAATGAGTACCCGC	24
BAC1080	<i>Bacteroides</i>	GCACTTAAGCCGACACCT	17
LGC354	Gram-positive bacteria with low G+C content	TGGAAGATTCCCTACTGC	36
HGC69A	Gram-positive bacteria with high G+C content	TATAGTTACCACCGCGT	44
MEB859	<i>Methanobacteriales</i> (except <i>Methanothermaceae</i>)	GGACTTAACAGCTTCCCT	9
MC1109	<i>Methanococcales</i>	GCAACATAGGGCACGGGTCT	43
MG1200	<i>Methanomicrobiales</i>	CGGATAATTCGGGGCATGCTG	43
MSSH859	<i>Methanosarcinales</i>	CTCACCCATACCTCACTCGGG	9
MS1414	<i>Methanosarcinales</i> (except <i>Methanosaeta</i>)	CTCACCCATACCTCACTCGGG	43
MX825	<i>Methanosaeta</i>	TCGCACCGTGGCCGACACCTAGC	43

Table 2.

Sequences from NCBI database with the highest similarity to each band. For uncultured microorganisms a brief description of the environment of origin is given.

Band ^a	P ^b	Closest relative (Accession number)	S ^c (%)
B1	c,m	<i>Syntrophobacter fumaroxidans</i> (X82874)	92
B2	i,c	Clone I79 (AY692039), this work	99
		<i>Oleomonas sagaranensis</i> (D45202)	97
B3	i,c	Uncultured IMCC1716 (DQ664239), freshwater bacteria	99
		<i>Azonexus fungiphilum</i> (AJ630292)	97
B4	c,m	Uncultured clone SsB12 (AB291302), UASB reactor	92
		<i>Hydrogenophaga defluvii</i> (AJ585993)	90
B5	i	Clone I73 (AY692051), this work	99
		<i>Flavobacterium frigidum</i> (AJ557887)	93
B6	c,m	Clone M77 (AY692049), this work	99
		<i>Catabacter hongkongensis</i> (AY574991)	91
B7	i	<i>Dechloromonas aromatica</i> (CP000089)	98
B8	c,m	Clone M78 (AY692048), this work	99
		<i>Aminobacterium colombiense</i> (AF069287)	90
B9	i,c	Clone BA128 (AF323770), methanogenic consortium	99
		<i>Thermovirga lienii</i> (DQ071273)	96
B10	i,c	Clone I92 (AY692047) this work	99
		<i>Arcobacter</i> sp. R-28314 (AM084114)	98
B11	i	<i>Rhodococcus opacus</i> (AY027583)	99
A1	c,m	Uncultured CLONG74 (DQ478747), anaerobic sludge	98
		<i>Metanosarcina mazei</i> (AY196685)	94
A2	c,m	Clone M1 (AY692055), this work	98
		<i>Methanosaeta concilli</i> (X51423)	96
A3	c,m	Uncultured methanospirillum (DQ478753), UASB reactor	100
		<i>Methanococcus palmolei</i> (Y16382)	95

563 ^{a)} A: *Archaea*, B: *Bacteria*

564 ^{b)} Period, i: initial, c: consolidation, m: mature

565 ^{c)} Similarity

566

Table 3.

Abundance of operational taxonomic units (OTUs) determined with each clone library and sequences from NCBI database with the highest similarity to each OTU. For uncultured microorganisms, a brief description of the environment of origin is given.

OTU ^a	P ^b	Abundance (%)	Closest relative (accession number)	S ^c (%)
<i>α-Proteobacteria</i>				
Cb1	c	16.7	<i>Oleomonas sagaranensis</i> (D45202)	97
Cb2	c	5.6	<i>Azospirillum brasilense</i> (X79733)	96
<i>β-Proteobacteria</i>				
Cb3	c	27.8	<i>Dechloromonas</i> sp. LT-1 (AY124797)	98
<i>δ-Proteobacteria</i>				
Cb4	m	36.3	Uncultured bacterium PL-37B10 (AY570628), oil reservoir.	99
<i>ε-Proteobacteria</i>				
Cb5	c	38.9	Uncultured <i>Arcobacter</i> sp. DS081 (DQ234164), mangrove bacterioplankton.	99
<i>Clostridia</i>				
Cb6	m	27.3	Uncultured bacterium CLONG96 (DQ478749), UASB reactor.	95
Cb7	m	18.2	Uncultured bacterium SJA-136 (AJ009493), anaerobic trichlorobenzene-transforming microbial consortium	96
Cb8	m	9.1	Uncultured bacterium SHA-74 (AJ306755), dechlorinate consortium	94
<i>Flavobacteria</i>				
Cb9	c	11.1	<i>Flavobacterium frigidarium</i> (AY771722)	93
<i>Thermotogae</i>				
Cb10	m	9.1	Uncultured bacterium (AB195923), anaerobic reactor.	99
<i>Methanomicrobia</i>				
Ca1	c	100	<i>Methanosaeta concilii</i> (X51423)	99
Ca2	m	91.7	<i>Methanosaeta concilii</i> (X51423)	98
Ca3	m	6.2	<i>Methanosarcina mazei</i> (AE008384)	98
Ca4	m	2.1	<i>Methanospirillum hungatei</i> (M60880)	96

568 ^{a)} Ca: *Archaea*, Cb: *Bacteria*

569 ^{b)} Period, c: consolidation, m: mature

570 ^{c)} Similarity

571 **FIGURE LEGENDS**

572 Figure 1. Micrographs of a biofilm over time using scanning electron microscopy. 1000x
573 magnification for all the pictures except for 60 days (200x). Details shown in the inner square
574 are 4000x. (B)

575

576 Figure 2. Growth curve of a biofilm during the first 10 days of development.

577

578 Figure 3. FISH of different development stages of a biofilm viewed by epifluorescence and CLS
579 microscopies. A, B, C, D, E and F: 36 hours. G, H and I: 4 days. J: 60 days. The samples A, B,
580 D, E, F, I were simultaneously stained with DAPI (blue) and specific-group Cy3-labeled probes
581 (red). (A) *α-Proteobacteria* (ALF338-Cy3). (B) *β-Proteobacteria* (BET42a-Cy3). (D) Sulfate-
582 reducing bacteria (SRB385-Cy3). (E) *Syntrophobacter* (SYN835-Cy3). (F) *Methanomicrobiales*
583 (MG1200-Cy3), with *Methanospirillum*-like red rods. (G) Overlay of *Methanobacteriales*
584 (MEB859-Cy3, red) and *Archaea* (ARC915-fluos, green). The samples C and H were
585 simultaneously hybridized with a bacterial probe (EUB338-fluos, green) and other probes: (C) *γ*-
586 *Proteobacteria* (GAM42a-Cy3, yellow) and (H) *Archaea* (ARC915-Cy3, red). (I) Detail of
587 *Methanosarcina* group (ARC915-Cy3). (J) Orthogonal CLMS section of the XZ plane of a mature
588 biofilm hybridized with specific probes for *Archaea* and *Bacteria* (ARC915-Cy3, red and
589 EUB338-fluos, green). All the micrographs have a 630x magnification with the exception of I
590 which has a 1000x magnification.

591

592 Figure 4. DGGE fingerprint for *Archaea* (A) and *Bacteria* (B) throughout the experiment.

593

594 Figure 5. Archaeal phylogenetic tree based on almost complete 16S rRNA gene sequences
595 retrieved from the cloning analysis. The bar scale represents 10 nucleotide substitutions per 100
596 nucleotides. The tree was constructed using parsimony.

597

598 Figure 6. Bacterial phylogenetic tree based on complete 16S rRNA gene sequences retrieved
599 from the cloning analysis. The bar scale represents 10 nucleotide substitutions per 100
600 nucleotides. The tree was constructed using parsimony.

601

602

603

604

605

606

607

608

609

610

611

612

613

614

615

616

617

618

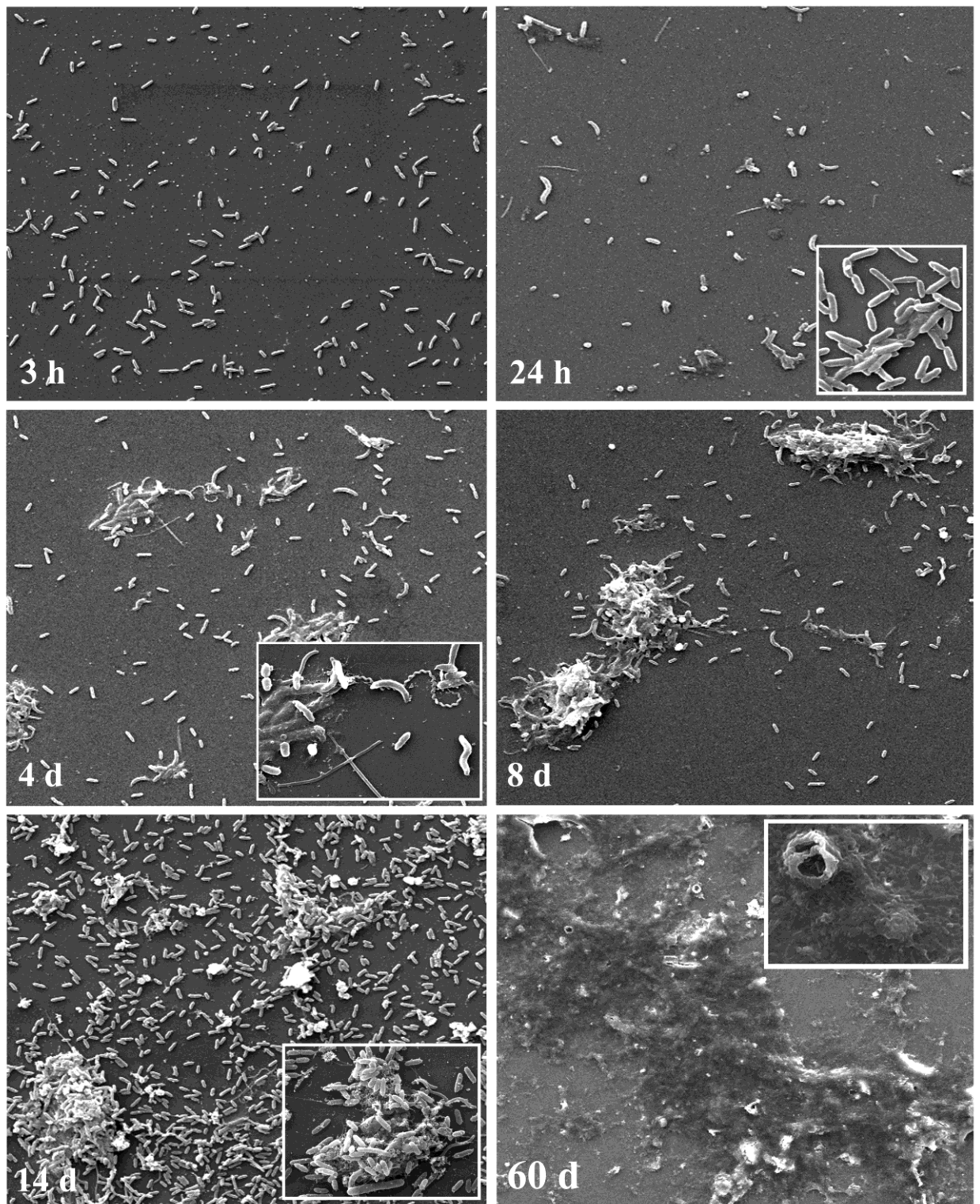
619

620

621

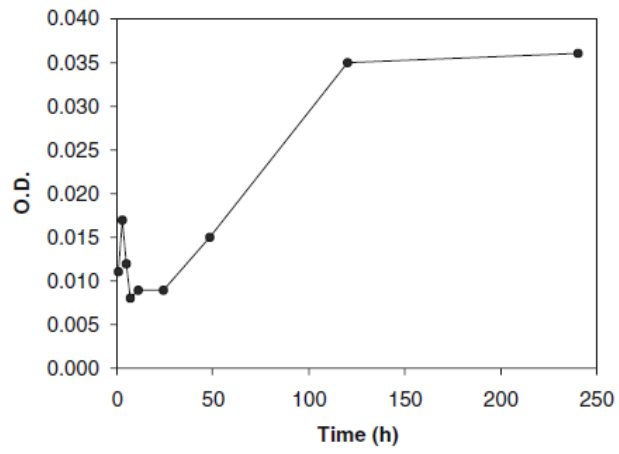
622

Figure 1



626

Figure 2



627

628

629

630

631

632

633

634

635

636

637

638

639

640

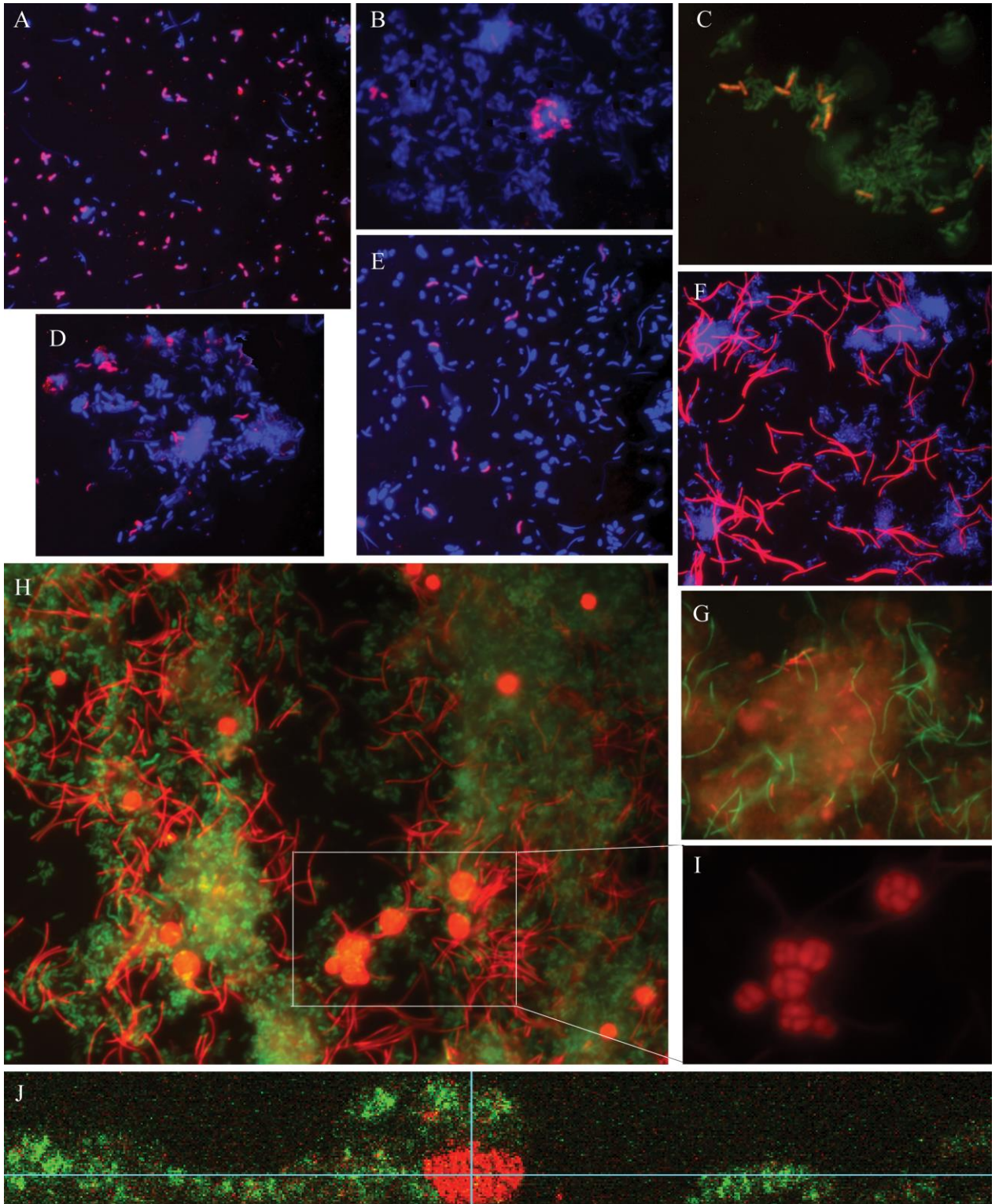
641

642

643

644

Figure 3

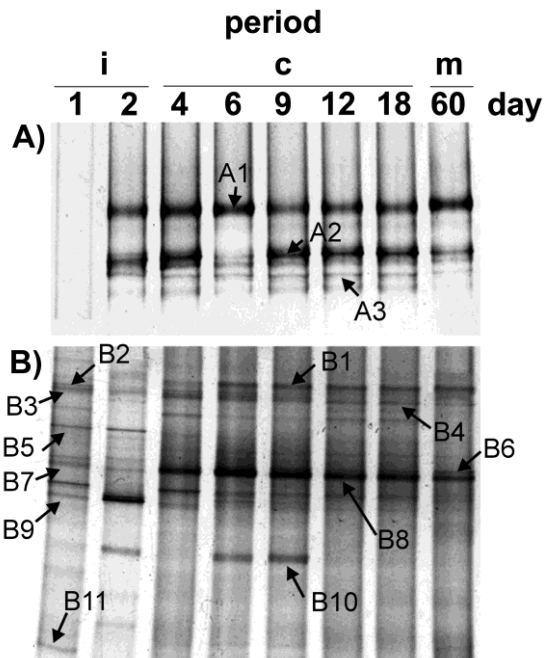


645

646

647

Figure 4



648

649

650

651

652

653

654

655

656

657

658

659

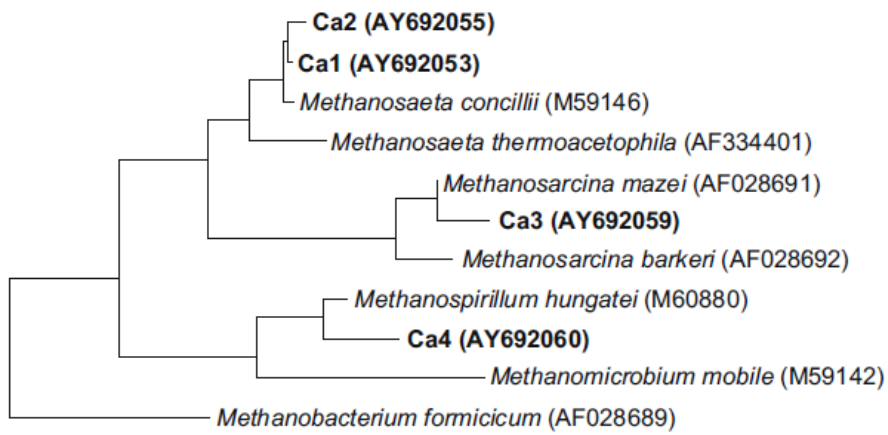
660

661

662

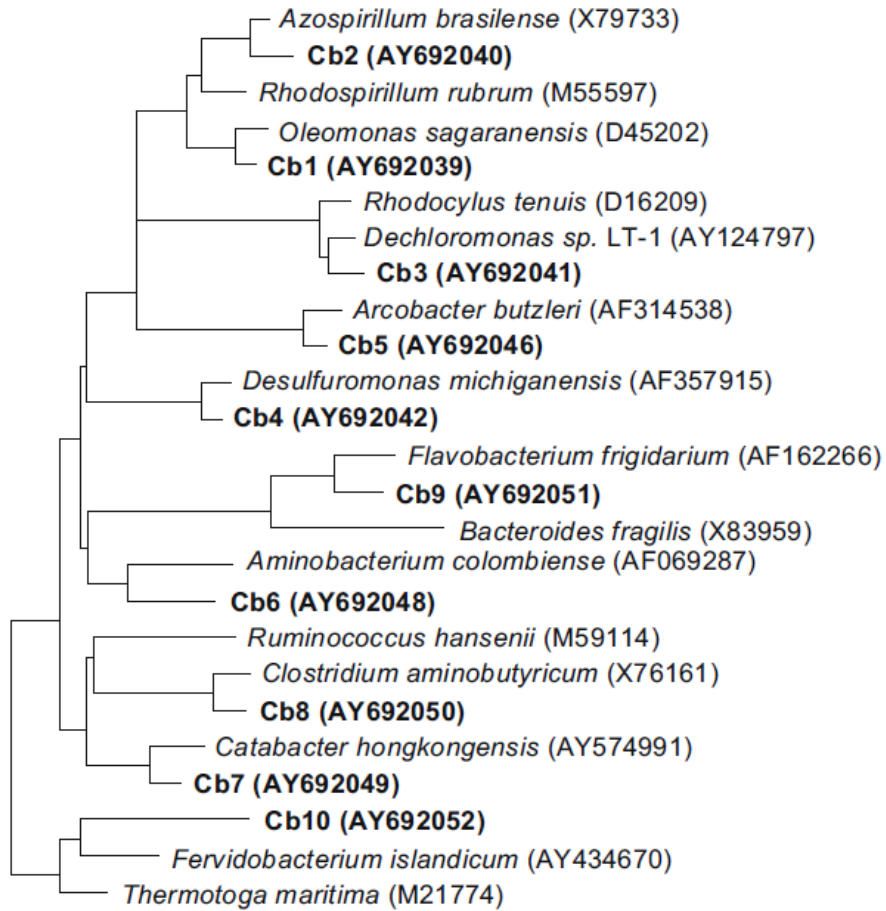
663

Figure 5



664
 665
 666
 667
 668
 669
 670
 671
 672
 673
 674
 675
 676
 677
 678
 679
 680
 681

Figure 6



682

0.10

683

684

685